orders, As(1)-S(1), 0.67; As(2)-S(1), 0.5; As(1)-S(2), As(2)-S(3), and As(2)-S(4), 1.17], as illustrated in Figure 7. It is interesting to note that the heteroatom interring bonds in the complexes **6** are in contrast to the observations made for the analogous phosphine-phosphenium complexes, in which a phosphorus-phosphorus bond is evident.[11,41]

Our initial theoretical assessment of simple phosphenium and arsenium models at 6-31g* and sto-3g* levels, respectively, has shown an overwhelming energetic preference for the monomeric species in each case, with respect to dimers of various conformations.[42] While theoretical studies continue, at this time we view the dimers **5** in terms of a mutual intermonomer HOMO-LUMO donation, recognizing that the HOMO of the cation is a π-MO entirely nitrogen based and the LUMO is principally arsenic based (also consistent with the observed structure for the complex **6**). The apparent avoidance of association by phosphenium cations is perhaps an indication of the more effective P-X π-interaction in the monomer.

Acknowledgment. This work has been supported by grants from the Natural Sciences and Engineering Research Council of Canada (N.B.), the donors of the Petroleum Research Fund, administered by the American Chemical Society (N.B.), and Dalhousie University. We thank Dr. Don Hooper and the Atlantic Region Magnetic Resonance Centre for use of the NMR facilities, Mr. Jürgen Müller for construction of the custom glass apparatus, and Mr. Derek Gates for assistance with some of the preparative aspects.

Supplementary Material Available: Tables of positional parameters, thermal parameters, bond lengths, and bond angles for **5a**$(AlCl_4)_2$, **5a**$(GaCl_4)_2$, **5b**$(GaCl_4)_2$, **6b**$(GaCl_4)$, and **4b** (13 pages); tables of observed and calculated structure factors (43 pages). Ordering information is given on any current masthead page.

(41) Schultz, C. W.; Parry, R. W. *Inorg. Chem.* **1976**, *15*, 3046. Cowley, A. H.; Lattman, M.; Wilburn, J. C. *Inorg. Chem.* **1981**, *20*, 2916. Baxter, S. G.; Collins, R. L.; Cowley, A. H.; Sena, S. F. *Inorg Chem.* **1983**, *22*, 3475.
(42) Boyd, R. J.; Burford, N.; MacKinnon, C. Unpublished results.

Stereodynamics of Isopropyldimethylamine. $^{13}C\{^1H\}$ and ^1H Dynamic NMR Studies. Molecular Mechanics Calculations

Jay H. Brown* and C. Hackett Bushweller*

Contribution from the Department of Chemistry, University of Vermont, Burlington, Vermont 05405-0125. *Received February 10, 1992*

Abstract: Since it is the simplest tertiary aliphatic amine that has one isopropyl group, isopropyldimethylamine (IDMA) is an important member of a group of simple aliphatic amines. Both the ^1H and $^{13}C\{^1H\}$ NMR spectra of IDMA are decoalesced into two subspectra at about 94 K due to slowing isolated rotation about the methine carbon-nitrogen bond. The major subspectrum is assigned to the enantiomeric conformations that have one isopropyl methyl group anti (A) and the other gauche (G) to the nitrogen lone pair (AG and GA forms). The minor subspectrum is assigned to the GG conformation that has both isopropyl methyl groups gauche to the lone pair. At about 94 K, there is a free energy preference for the AG (or GA) conformation over the GG equal to 0.070 ± 0.020 kcal/mol. Simulations of the exchange-broadened NMR spectra indicate that the AG (or GA) to GG conformational exchange occurs at a faster rate than the AG to GA process. The latter process is sufficiently slower that it contributes little to exchange broadening of the NMR line shape. The free energy of activation ($\Delta G^\ddagger$) for the faster NMR-visible AG (or GA) to GG conversion is 4.5 ± 0.1 kcal/mol at 95 K. This barrier is among the lowest measured by using the NMR method. The lower limit for $\Delta G^\ddagger$ associated with the AG to GA process is 5.2 kcal/mol at 95 K. Molecular mechanics calculations of conformational energies and rotation barriers agree well with the experimental data. The molecular mechanics calculations indicate a small enthalpy preference for the GG conformation (0.19 kcal/mol) and a barrier for the AG to GA conversion ($\Delta H^\ddagger$ = 7.84 kcal/mol) that is higher than that for the AG (or GA) to GG process (5.37 kcal/mol).

Introduction

Any successful attempt to elucidate a comprehensive picture of the stereodynamics of an aliphatic amine requires identification of the equilibrium conformations and the preferred pathways for conformational exchange.[1] Two different types of internal motion are relevant. One is pyramidal inversion at nitrogen.[2] The other involves isolated rotation about various bonds in the amine.[3] In many simple aliphatic amines, the rotation-inversion dichotomy is clearly delineated; the energy barrier for inversion is significantly greater than that for any isolated rotation process.[4] Infrared spectroscopy, microwave spectroscopy, and molecular orbital calculations have shed considerable light on the stereodynamics of simple aliphatic amines including methylamine,[5] dimethylamine,[5a,6] trimethylamine,[5a,7] ethylamine,[8] isopropylamine,[8d,9]

(1) Bushweller, C. H. In *Acyclic Organonitrogen Stereodynamics*; Lambert, J. B., Takeuchi, Y., Eds.; VCH Publishers: New York, 1992.
(2) Lambert, J. B. *Top. Stereochem.* **1971**, *6*, 19. Lehn, J. M. *Fortschr. Chem. Forsch.* **1970**, *15*, 311. Payne, P. W.; Allen, L. C. In *Applications of Electronic Structure Theory*; Schaefer, H. F., Ed.; Plenum Press: New York, 1977; Vol. 4.
(3) Orville-Thomas, W. J., Ed. *Internal Rotation in Molecules*; J. Wiley and Sons: New York, 1974.
(4) Bushweller, C. H.; Fleischman, S. H.; Grady, G. L.; McGoff, P.; Rithner, C. D.; Whalon, M. R.; Brennan, J. G.; Marcantonio, R. P.; Domingue, R. P. *J. Am. Chem. Soc.* **1982**, *104*, 6224.
(5) (a) Eades, R. A.; Weil, D. A.; Dixon, D. A.; Douglass, C. H., Jr. *J. Phys. Chem.* **1981**, *85*, 976. (b) Flood, E.; Pulay, P.; Boggs, J. E. *J. Am. Chem. Soc.* **1977**, *99*, 5570. (c) Tsuboi, M.; Hirakawa, A. Y.; Takamitsu, I.; Sasaki, T.; Tamagake, K. *J. Chem. Phys.* **1964**, *41*, 2721. (d) Tsuboi, M.; Hirakawa, A. Y.; Tamagake, K. *J. Mol. Spectrosc.* **1967**, *22*, 272. (e) Nishikawa, T.; Itoh, T.; Shimoda, K. *J. Chem. Phys.* **1955**, *23*, 1735.
(6) Wollrab, J. E.; Laurie, V. W. *J. Chem. Phys.* **1968**, *48*, 5058. Wollrab, J. E.; Laurie, V. W. *J. Chem. Phys.* **1971**, *54*, 539.
(7) Weston, R. E., Jr. *J. Am. Chem. Soc.* **1954**, *76*, 2645. Lide, D. R.; Mann, D. E. *J. Chem. Phys.* **1958**, *28*, 572.
(8) (a) Durig, J. R.; Li, Y. S. *J. Chem. Phys.* **1975**, *63*, 4110. (b) Tsuboi, M.; Tamagake, K.; Hirakawa, A. Y.; Yamaguchi, J.; Nakagawa, H.; Manocha, A. S.; Tuazon, E. C.; Fateley, W. G. *J. Chem. Phys.* **1975**, *63*, 5177. (c) Hamada, Y.; Hashiguchi, K.; Hirakawa, A. Y.; Tsuboi, M.; Nakata, M.; Tasumi, M.; Kato, S.; Morokuma, K. *J. Mol. Spectrosc.* **1983**, *102*, 123. (d) Alsenoy, C. V.; Scarsdale, J. N.; Williams, J. O.; Schaefer, L. J. *J. Mol. Struct.* **1982**, *86*, 365. (e) Krueger, P. J.; Jan, J. *Can. J. Chem.* **1970**, *48*, 3229.
(9) Bohlmann, F. *Chem. Ber.* **1958**, *91*, 2157. Hamlow, H. P.; Okada, S.; Nakagawa, N. *Tetrahedron Lett.* **1964**, 2553.

0002-7863/92/1514-8153$03.00/0

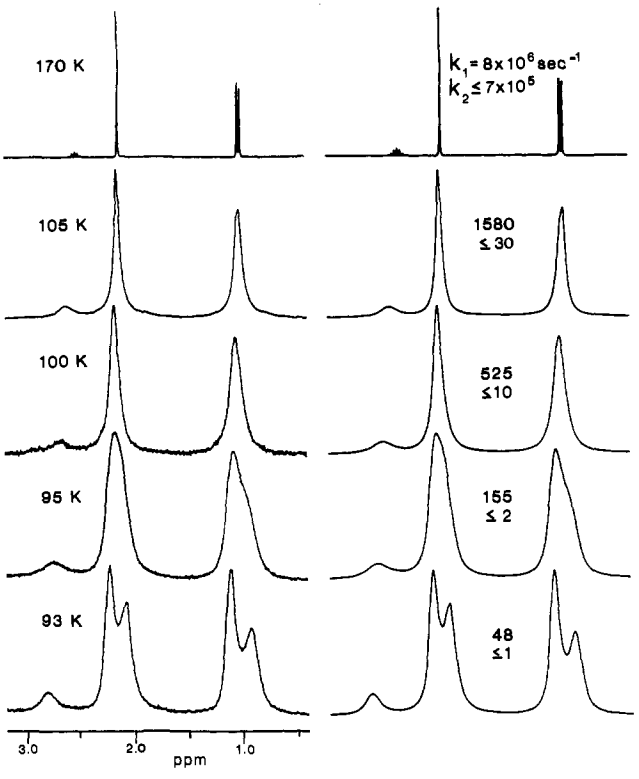

Figure 1. Experimental ^{1}H DNMR spectra (250.136 MHz) of isopropyldimethylamine (3% v/v in $CBrF_3$) in the left column and theoretical simulations in the right column. The rate constants are defined in eq 1. All of the theoretical spectra shown were computed by setting k_2 equal to zero. The value of k_2 listed at 93, 95, or 100 K is the upper limit that still gives an acceptable fit of the experimental spectrum. Values of k_2 greater than the value listed at each temperature give unacceptable results. The listed values of k_2 at 105 and 170 K were obtained by a least squares extrapolation.

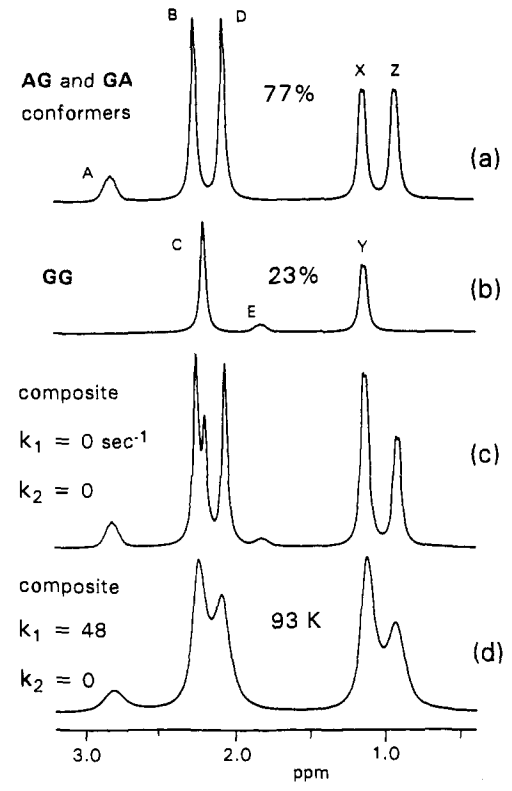

Figure 2. Decomposition of the theoretical simulation of the ^{1}H NMR spectrum of isopropyldimethylamine at 93 K. The upper three spectra are computed with all rate constants equal to zero: (a) subspectrum due to the AG and GA conformations in eq 1; (b) subspectrum due to the GG conformation; (c) composite spectrum resulting from the superposition of the upper two subspectra; (d) composite spectrum calculated by using $k_1 = 48$ s^{-1} and $k_2 = 0$ that gives a fit to the experimental spectrum at 93 K.

ethylmethylamine,[8c,10] and dimethylethylamine.[11] Dynamic nuclear magnetic resonance (DNMR) spectroscopy used in conjunction with molecular mechanics calculations revealed detailed pictures of the stereodynamics of simple trialkylamines including diethylmethylamine,[4] triethylamine,[4] dibenzylmethylamine,[1] tribenzylamine,[12] and 2-butylethylmethylamine.[13] In the more sterically crowded *tert*-butylethylmethylamine, there is no dichotomy between inversion and rotation; *concomitant* inversion and rotation is the preferred itinerary for conformational exchange.[14] In highly encumbered trialkylamines such as $(CH_3CH_2)_2CHN(i\text{-}C_3H_7)_2$ and $(t\text{-}C_4H_9)_2CHN(CH_3)_2$, there are remarkably large barriers to rotation about the methine carbon–nitrogen bonds on a trivalent nitrogen template that is close to being or is actually trigonal planar.[15,16] Gas-phase electron diffraction studies indicate that the equilibrium conformation of triisopropylamine deviates only slightly from C_{3h} symmetry with an almost planar NC_3 template and all three methine carbon–hydrogen bonds in the plane.[17] In these sterically crowded systems, either the inversion barrier is minuscule or, as a result of a trigonal planar nitrogen, the inversion process is irrelevant.

While some attention has been paid to isopropylamine and a few derivatives,[1,8d,9,15,17] relatively little is known about the stereodynamics of isopropylamines. Isopropyldimethylamine (IDMA) is the simplest tertiary aliphatic amine that has one isopropyl group and must be considered an important member of the family of isopropylamine derivatives. In this paper, we report both DNMR and molecular mechanics studies of IDMA. Both the ^{1}H and $^{13}C\{^1H\}$ NMR spectra of IDMA decoalesce at very low temperatures in response to slowing rotation about the methine carbon–nitrogen bond and reveal the presence of three equilibrium conformations (two C_1-symmetric enantiomers and a C_s-symmetric achiral form). Theoretical simulations of the DNMR spectra reveal a preferred pathway for conformational exchange that involves interconversion of the C_1 forms via the C_s conformer. This process has one of the lowest energy barriers (4.5 kcal/mol) measured by using the DNMR method. Molecular mechanics calculations of equilibrium conformational energies and rotation barriers are in good agreement with the experimental results.

DNMR Studies and Discussion

The ^{1}H NMR spectrum (250.136 MHz) of IDMA (3% v/v in $CBrF_3$) at 170 K shows a septet (δ 2.54, $^3J_{HCCH}$ = 6.7 Hz, CH), a doublet (δ 1.02, $C(CH_3)_2$), and a singlet (δ 2.14, $N(CH_3)_2$). Below 105 K, the spectrum decoalesces and, at 93 K, shows five resolved resonances (Figure 1). A significant rate of conformational exchange and efficient transverse relaxation (T_2) obscures observation of the scalar coupling in the 93 K spectrum. The sample froze at 92 K. In sterically unencumbered aliphatic amines such as IDMA, rotation barriers about C–CH_3 and N–CH_3 bonds are invariably too low to be DNMR-visible.[4] The decoalescence shown in Figure 1 is not due to isolated methyl rotation. The barrier to inversion in IDMA should be close to that already determined for isopropylethylmethylamine (7.5 kcal/mol).[18] The

(10) Durig, J. R.; Compton, D. A. *J. Phys. Chem.* **1979**, *83*, 2873. Penn, R. E.; Boggs, J. E. *J. Mol. Spectrosc.* **1973**, *47*, 340. Allinger, N. L.; Burkert, U.; Profeta, S., Jr. *J. Comput. Chem.* **1980**, *1*, 281.
(11) Durig, J. R.; Cox, F. O. *J. Mol. Struct.* **1982**, *95*, 85.
(12) Fleischman, S. H.; Whalon, M. R.; Rithner, C. D.; Grady, G. L.; Bushweller, C. H. *Tetrahedron Lett.* **1982**, 4233.
(13) Danehey, C. T., Jr.; Grady, G. L.; Bonneau, P. R.; Bushweller, C. H. *J. Am. Chem. Soc.* **1988**, *110*, 7269.
(14) Bushweller, C. H.; Anderson, W. G.; Stevenson, P. E.; Burkey, D. L.; O'Neil, J. W. *J. Am. Chem. Soc.* **1974**, *96*, 3892.
(15) Lunazzi, L.; Macciantelli, D.; Grossi, L. *Tetrahedron* **1983**, *39*, 305.
(16) Berger, P. A.; Hobbs, C. F. *Tetrahedron Lett.* **1978**, 1905.
(17) Bock, H.; Coebel, I.; Havlas, Z.; Liedle, S.; Oberhammer, H. *Angew. Chem., Int. Ed. Engl.* **1991**, *30*, 187.

decoalescence illustrated in Figure 1 is associated with a much lower barrier process. With inversion very slow on the NMR chemical-exchange time scale below 130 K, the DNMR behavior in Figure 1 must be assigned to slowing isolated rotation about the methine carbon–nitrogen bond. In fact, the inherent molecular symmetry of IDMA and the ordering of the inversion and isolated rotation barriers in IDMA renders nitrogen inversion invisible to the DNMR method.[1]

The 93 K spectrum is simulated accurately by superimposing two subspectra.[19] A decomposition of the theoretical simulation is shown in Figure 2. The upper two subspectra in Figure 2 are added to produce the composite spectrum for which all rates of exchange are zero. The top three spectra were computed by using the same T_2 values employed in the simulation of the experimental spectrum at 93 K. The bottom composite spectrum incorporates an exchange rate (vide infra) that gives an excellent fit to the experimental spectrum at 93 K. Each methyl group resonance is simulated accurately as three identical proton chemical shifts; rotation about C–CH_3 and N–CH_3 bonds is fast even at 93 K. The major subspectrum (77%) includes a methine proton signal at δ_A 2.82 ($^3J_{HCCH}$ = 6.7 Hz), two isopropyl methyl doublets of equal area at δ_X 1.13 and δ_Z 0.92, and two *N*-methyl singlets of equal area at δ_B 2.26 and δ_D 2.07. This subspectrum is shown at the top of Figure 2. The minor subspectrum (23%) includes a methine proton resonance at δ_E 2.00 ($^3J_{HCCH}$ = 6.7 Hz), one isopropyl methyl doublet at δ_Y 1.13, and one *N*-methyl singlet at δ_C 2.20. The presence of a methine proton resonance at δ_E 2.00 is inferred from the total line-shape simulation. This was verified by examination of the ^{1}H DNMR spectra of $(CH_3)_2CHN(CD_3)_2$ in $CBrF_3$ (3% v/v). At 92 K, the deuterated derivative shows a decoalescence of the methine proton signal into two differentially populated resonances. Minor signals due to the isotopic impurity $(CH_3)_2CHN(CHD_2)_2$ overlap the minor lower frequency methine proton resonance. In the computation of a theoretical spectrum at 92 K, an appropriate adjustment of signal intensities was necessary to account for the isotopic impurity. The spectrum of the deuterated derivative at 92 K is simulated accurately by using the same magnetization-exchange model employed in Figure 1, and an accurate fit confirmed the presence of two methine proton resonances at δ 2.82 (77%) and δ 2.00 (23%).

The major subspectrum in Figure 2 is rigorously consistent with the C_1 symmetry of the enantiomeric AG and GA conformers in eq 1. In either conformer, the isopropyl methyl groups are

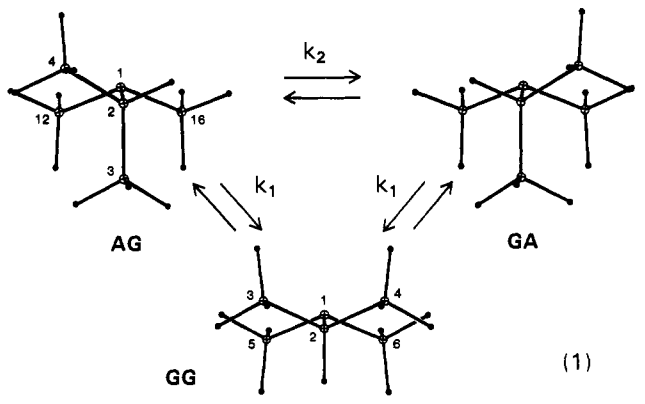

(1)

diastereotopic. One is vicinal and anti (A) to the nitrogen lone pair; the other is vicinal and gauche (G) to the lone pair. On the basis of well-established ^{1}H chemical shift correlations for methyl groups that are vicinal to the nitrogen lone pair in tertiary aliphatic amines, the resonance at δ_Z 0.92 is assigned to the A methyl group and the signal at δ_X 1.13 to the G methyl.[14] In the AG and GA forms, the *N*-methyl groups are diastereotopic, consistent with the observation of two *N*-methyl singlets at δ_B 2.26 and δ_D 2.07. At 93 K, there is 38.5% of each enantiomer.

The minor subspectrum is rigorously consistent with the C_s symmetry of the GG conformation (eq 1). The isopropyl methyl groups are enantiotopic. The *N*-methyl groups are enantiotopic. The 0.8 ppm shift of the methine proton signal to lower frequency, as compared to that of the AG and GA forms, is consistent with a methine proton that is anti to the lone pair.[4] At 93 K, there is 23% of the GG conformer. At 93 K, the AG (or GA) conformer is preferred over the GG form by a free energy difference equal to 0.095 kcal/mol.

Simulations of the DNMR spectra led inexorably to a preferred magnetization-exchange model. For the *N*-methyl resonances, accurate simulations can be achieved by using a B_3D_3 to C_6 to D_3B_3 magnetization-exchange pathway with *no direct* B_3D_3 to D_3B_3 exchange (Figure 2). This implies that the B_3D_3 to D_3B_3 transfer either is not occurring or is occurring at a sufficiently slower rate than other processes that it has little effect on the DNMR line shape. The rate constant k_1 in Figure 1 is associated with the B_3D_3 (or D_3B_3) to C_6 transfer of magnetization and corresponds to the AG (or GA) to GG conformational exchange (eq 1). The rate constant k_2 is associated with the B_3D_3 to D_3B_3 exchange and corresponds to the AG to GA enantiomerization. For the isopropyl groups, accurate simulations can be achieved by using an AX_3Z_3 to EY_6 to AZ_3X_3 transfer with *no direct* AX_3Z_3 to AZ_3X_3 exchange. The rate constant k_1 in Figure 1 is also associated with the AX_3Z_3 (or AZ_3X_3) to EY_6 transfer and k_2 with the AX_3Z_3 to AZ_3X_3 exchange. Even at 93 K, it is necessary to employ a significant rate of exchange (Figure 1). According to this model, the free energy of activation ($\Delta G^\ddagger$) for the AG (or GA) to GG conversion is 4.4 ± 0.1 kcal/mol at 95 K. All of the theoretical spectra illustrated in Figure 1 were computed by setting k_2 equal to zero. In an attempt to place a lower limit on $\Delta G^\ddagger$ for the AG to GA process, additional theoretical spectra were calculated by keeping k_1 constant and progressively increasing k_2 until there was a clearly discernible discrepancy between the theoretical and experimental spectra. The upper limit for k_2 that still produces an acceptable fit at 93, 95, or 100 K is listed in Figure 1. Any value above each of the listed values gives unacceptable results. The values of k_2 at 105 and 170 K were obtained by a least squares extrapolation. Any attempt to use equal values for k_1 and k_2 gave clearly unacceptable results. At 95 K, the upper limit on k_2 is 2 s^{-1}, giving a lower limit on $\Delta G^\ddagger$ of 5.2 kcal/mol. The k_1 process (eq 1) is faster than the k_2 conversion.

The inescapable conclusion is that the AG (or GA) to GG conformational exchange in IDMA occurs at a faster rate than the AG to GA exchange. Intuitively, a slower rate for the AG to GA process is consistent with two C–CH_3/N–CH_3 and one C–H/lone pair eclipsing interactions in the transition state that lead to a higher barrier than that associated with the AG (or GA) to GG process. In the less sterically crowded transition state for the latter process, there are one C–CH_3/N–CH_3 eclipsing, one C–H/N–CH_3 eclipsing, and one C–CH_3/lone pair eclipsing interactions.

The $^{13}C\{^1H\}$ NMR spectrum (62.898 MHz) of IDMA (3% v/v in $CBrF_3$) at 180 K (Figure 3) shows three singlets at δ 55.80 (methine carbon), δ 41.50 (*N*-methyl carbons), and δ 18.76 (isopropyl methyl carbons). Below 120 K, both the *N*-methyl and isopropyl methyl signals decoalesce and, at 95 K, each shows two well-resolved signals of different intensities (Figure 3). At 95 K, the methine carbon resonance shows the onset of decoalescence but is still significantly exchange-broadened. In a manner strictly analogous to the ^{1}H DNMR spectra, the $^{13}C\{^1H\}$ DNMR spectra are simulated accurately by the superposition of two subspectra. In the major subspectrum (72%), there is a methine carbon resonance at δ_B 54.06, two *N*-methyl signals of equal area at δ_L 44.87 and δ_N 35.45, and two isopropyl methyl singlets of equal area at δ_X 23.82 and δ_Z 14.23. This subspectrum is shown at the top of Figure 4. The minor subspectrum (28%) includes a methine carbon signal (δ_A 56.54), one *N*-methyl resonance (δ_M 44.87), and one isopropyl methyl resonance (δ_Y 23.78) and is illustrated second from the top in Figure 4. The composite spectrum under con-

(18) Bushweller, C. H.; Wang, C. Y.; Reny, J.; Lourandos, M. Z. *J. Am. Chem. Soc.* **1977**, *99*, 3938.
(19) Bushweller, C. H.; Letendre, L. J.; Brunelle, J. A.; Bilofsky, H. S.; Whalon, M. R.; Fleischman, S. H. *QCPE* **1983**, Program No. 466.

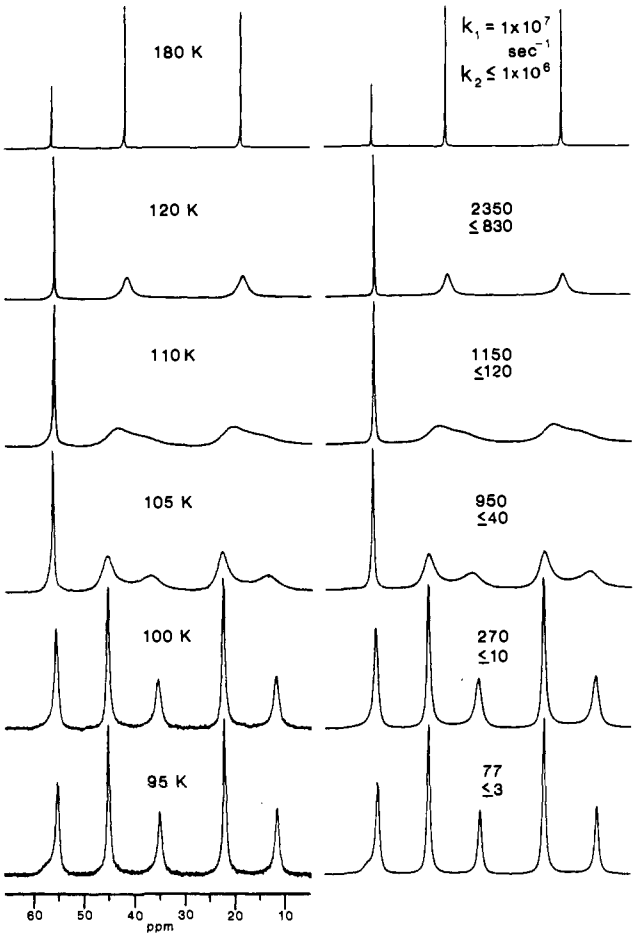

Figure 3. Experimental $^{13}C\{^1H\}$ DNMR spectra (62.898 MHz) of isopropyldimethylamine (3% v/v $CBrF_3$) in the left column and theoretical simulations in the right column. The rate constants are defined in eq 1. All of the theoretical spectra shown were computed by setting k_2 equal to zero. The value of k_2 listed at 95, 100, 105, or 110 K is the upper limit that still gives an acceptable fit of the experimental spectrum. Values of k_2 greater than the value listed at each temperature give unacceptable results. The listed values of k_2 at 120 and 180 K were obtained by a least squares extrapolation.

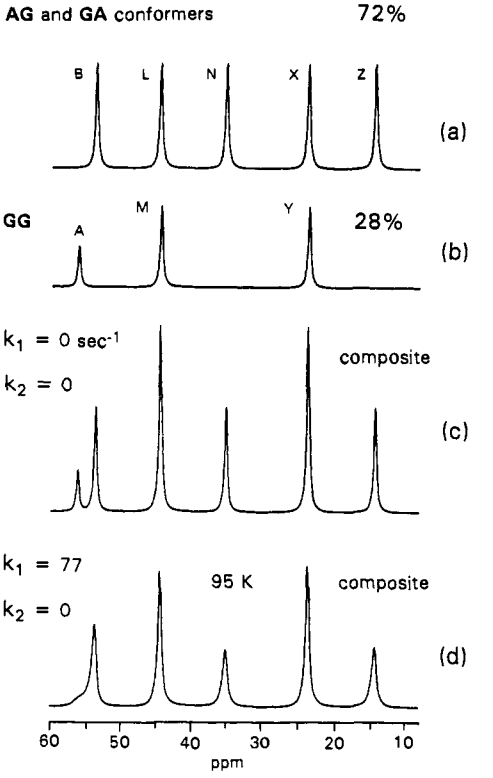

Figure 4. Decomposition of the theoretical simulation of the $^{13}C\{^1H\}$ NMR spectrum of isopropyldimethylamine at 95 K. The format for presentation of the subspectra and composite spectra is identical to that in Figure 2.

ditions of no exchange and the composite spectrum computed at an exchange rate that gives an accurate fit of the 95 K spectrum are also shown in Figure 4.

The major subspectrum is clearly consistent with the C_1 symmetry of the AG and GA enantiomers and accounts for 72% of the integrated intensity of the composite spectrum, in good agreement with the ^1H NMR data. The minor subspectrum (28%) reflects the C_s symmetry of the GG form and has an integrated intensity also in good agreement with the ^1H NMR data. From these data, the free energy preference for the AG conformer over the GG form is 0.048 kcal/mol at 95 K.

The ^{13}C NMR chemical shifts of the G isopropyl methyl groups in the GG (δ 23.78) and AG or GA (δ 23.82) conformations are essentially identical. However, the A isopropyl methyl carbon that is gauche to two *N*-methyl groups in the AG or GA conformation is significantly shielded (δ 14.23) relative to the G counterpart. The chemical shifts of an *N*-methyl carbon that is gauche to the methine proton and an isopropyl methyl group in the AG, GA, and GG forms are identical (δ 44.87). In contrast, the *N*-methyl carbon that is gauche to both isopropyl methyl groups in the C_1 conformers is significantly shielded (δ 35.45). It is interesting to note that the respective differences in chemical shift between the diastereotopic isopropyl methyl groups and the diastereotopic *N*-methyl groups are virtually identical.

Accurate simulations of the $^{13}C\{^1H\}$ DNMR spectra of the isopropyl group can be achieved by employing a BXZ to AY_2 to BZX magnetization-exchange pathway with no direct BXZ to BZX transfer (Figure 4). In Figure 3, k_1 is associated with the BXZ (or BZX) to AY_2 transfer [AG (or GA) to GG] and k_2 with the direct BXZ to BZX process (AG to GA). For the *N*,*N*-dimethyl resonances, an LN to M_2 to NL exchange with no direct LN to NL transfer gives accurate fits of the spectra; k_1 is associated with the LN (or NL) to M_2 process, and k_2, with the direct LN to NL exchange. The $^{13}C\{^1H\}$ DNMR spectra corroborate the preferred AG to GG to GA conformational-exchange pathway in IDMA. The free energy of activation for the AG (or GA) to GG conformational exchange derived from these simulations of the $^{13}C\{^1H\}$ DNMR spectra is 4.5 ± 0.1 kcal/mol at 110 K, in good agreement withh the ^1H DNMR results. While one must always be aware of systematic errors in DNMR line-shape analyses, the magnetization-exchange model described above gives a low entropy of activation equal to 0 ± 3 cal/(mol K). All of the theoretical spectra shown in Figure 3 were computed by setting k_2 equal to zero. By use of the approach described previously for the ^1H DNMR spectra, an upper limit for k_2 was estimated at each temperature, and this value is given in Figure 3. The estimated lower limit for the $\Delta G^{\ddagger}$ value associated with the AG to GA process is 5.2 kcal/mol at 100 K.

It is noteworthy that the rate constants derived from fits of the ^1H and $^{13}C\{^1H\}$ DNMR spectra are not exactly equal at the same temperatures (Figures 1 and 3). This could be due to errors in temperature measurement in two different NMR probes. The discrepancies could also result from the onset of slowing isolated rotation for a number of diastereotopic methyl groups. Slowing isolated methyl rotation will affect only the ^1H DNMR line shape. The magnetization-exchange model used to simulate the ^1H DNMR spectra cannot account for any additional exchange broadening due to slowing isolated methyl rotation. In the application of the magnetization-exchange model above, line broadening due to the early onset of slowing methyl rotation could be treated by using smaller effective T_2 values. This would compromise the accuracy of the rate constants derived from the simulations and could account for the discrepancy between the ^1H and $^{13}C\{^1H\}$ values. Molecular mechanics calculations for IDMA (vide infra) indicate that isolated methyl rotation barriers

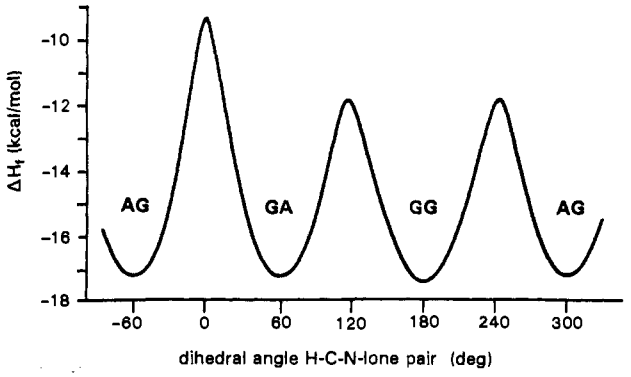

Figure 5. Energy profile for rotation about the methine carbon–nitrogen bond of isopropyldimethylamine calculated by using the general dihedral angle driver option in Allinger's MM2(87) molecular mechanics force field.[20] The H–C–N–(lone pair) dihedral angle is plotted on the horizontal axis.

Table I. Selected Dihedral Angles, Bond Angles, and Bond Lengths for the AG and GG Conformations (Eq 1) of Isopropyldimethylamine Calculated by Using Allinger's MM2(87) Molecular Mechanics Force Field

dihedral angle (deg)		bond angle (deg)		bond length (Å)	
		AG Conformer[a]			
3–2–1–12	61.8	3–2–4	109.6	1–12	1.456
3–2–1–16	−64.0	12–1–16	109.9	1–16	1.457
4–2–1–12	−64.3	2–1–12	114.0	1–2	1.466
4–2–1–16	170.0	2–1–16	112.3	2–4	1.541
		1–2–3	115.4	2–3	1.539
		1–2–4	111.7		
		GG Conformer[a]			
3–2–1–5	−57.6	5–1–6	109.2	1–5	1.458
4–2–1–6	57.5	2–1–5	112.3	1–6	1.458
3–2–1–6	179.0	2–1–6	112.3	1–2	1.469
4–2–1–5	−179.0	1–2–4	112.1	2–3	1.543
		1–2–3	112.1	2–4	1.543
		3–2–4	107.8		

[a] The atomic numbering scheme is given on the AG and GG Conformations shown in eq 1.

can be as high as 4.24 kcal/mol and that these processes could be sufficiently slow at 95 K to contribute to exchange broadening of the ^{1}H DNMR spectra.

Molecular Mechanics Calculations

A 360° general dihedral angle driver calculation (1° increments, NDRIVE = 1) for isolated rotation about the methine carbon–nitrogen bond in one invertomer of IDMA was performed by using the MM2(87) molecular mechanics program, which employs the Allinger–Profeta force field for aliphatic amines.[20] The resulting energy profile is shown in Figure 5. There are three energy minima corresponding to the AG, GA, and GG equilibrium conformations. For each equilibrium conformation, the geometry was optimized by using the standard Newton–Raphson energy minimization scheme. Selected bond lengths, bond angles, and dihedral angles for the AG and GG forms are compiled in Table I. For the AG and GA forms, the calculated heat of formation ($\Delta H°_f$) is −17.20 kcal/mol. For the GG conformation, $\Delta H°_f$ = −17.39 kcal/mol. The molecular mechanics calculations indicate a small *enthalpy* preference for the GG conformer (0.19 kcal/mol), while the NMR data show a small *free energy* preference for the AG (or GA) form (0.07 ± 0.02 kcal/mol). The NMR data might reflect a small entropy preference (≈3 cal/(mol K)) for either one of the C_1-symmetric forms over the C_s species. The apparent entropy preference for the C_1-symmetric conformation is more than twice that based on the entropy of mixing. In any event,

(20) Allinger, N. L. *QCPE* **1987**, Program No. MM2(87). Profeta, S., Jr.; Allinger, N. L. *J. Am. Chem. Soc.* **1985**, *107*, 1907.

Table II. Barriers to Isolated Methyl Rotation in the AG and GG Conformations of Isopropyldimethylamine Calculated by Using the Dihedral Angle Driver Option in Allinger's MM2(87) Molecular Mechanics Force Field[a]

conformn	methyl group[b]	$\Delta H^‡$ (kcal/mol)	conformn	methyl group[b]	$\Delta H^‡$ (kcal/mol)
AG	C3	2.96	GG	C3	3.18
	C4	3.24		C5	4.21
	C16	4.24			
	C12	4.06			

[a] The MM2(87)-calculated methyl rotation barrier in trimethylamine is 4.37 kcal/mol. The experimental value is 4.41 kcal/mol.[5a,7] [b] The atomic numbering scheme is given on the AG and GG conformations shown in eq 1.

the agreement between calculated and experimental energy differences is very good.

A perusal of Table I shows that the CH_3–N–CH_3 bond angles increase only slightly beyond the ideal value (107.7°), while the CH_3–N–CH bond angles open significantly, presumably in response to nonbonded repulsions. It is noteworthy that the C3–C2–N bond angle associated with the A isopropyl methyl group in the AG conformation opens significantly as compared to the ideal value (108.8°). This is analogous to the equilibrium conformation of methylamine, in which the pseudo-C_3 axis of the methyl group is tilted 3.5° toward the lone pair.[5] In methylamine, ab initio molecular orbital calculations assign the origin of the tilt to vicinal nonbonded repulsions involving the two amino protons and the methyl proton that is anti to the lone pair.[5] In an analogous manner, the tilt of the isopropyl group in IDMA could be assigned to nonbonded repulsions between the A methyl group and the *N*-methyl groups. While one must be cognizant of the parameterization of the lone pair as a pseudoatom, which tends to overestimate pyramidality at nitrogen, the MM2 force field calculates significant pyramidality at nitrogen. The dihedral angles associated with the isopropyl group (Table I) indicate classical staggering of vicinal substituents along the N–CH bond consistent with the calculated pyramidality at nitrogen. Significant pyramidality at nitrogen would serve to stabilize the GG conformation as compared to more sterically crowded systems in which pyramidality is decreased. In these less pyramidal molecules, enhanced vicinal nonbonded repulsions destabilize GG-type conformations relative to AG analogues.[16,17,21]

The dihedral angle driver calculation for rotation about the methine carbon–nitrogen bond provides calculated barriers ($\Delta H^‡$) for conformational exchange (Figure 5). For the direct AG to GA conversion, the MM2 barrier is 7.84 kcal/mol. The transition state has C_s symmetry with the C–H bond eclipsing the lone pair and a small C–N–C–C dihedral angle (−0.4°) for each of the two pairs of almost perfectly eclipsed C–C and N–C bonds. For the AG (or GA) to GG conversion, the calculated barrier is 5.37 kcal/mol. In the C_1-symmetric transition state, one C–C bond perfectly eclipses an N–C bond. The C–N–C–C dihedral angle is −0.06°. The other C–C bond partially eclipses the lone pair (dihedral angle C–C–N–(lone pair) = −8.9°). The H–C–N–C dihedral angle associated with the eclipsed C–H and N–C bonds is +1.7°. Consistent with the conclusions derived from the DNMR studies, the molecular mechanics force field indicates a barrier for the AG to GA rate process that is 2.47 kcal/mol higher than that for the AG (or GA) to GG conversion (Figure 5). The faster DNMR-visible AG (or GA) to GG process has a DNMR-measured free energy of activation equal to 4.5 kcal/mol. The lower limit assigned to $\Delta G^‡$ for the slower AG to GA process is 5.2 kcal/mol. While the dihedral angle driver calculations overestimate the barrier magnitudes, the barrier ordering agrees with the DNMR results.

In order to fully elucidate the stereodynamics of IDMA, barriers to isolated methyl rotation for all the diastereotopic methyl groups

(21) Rithner, C. D.; Bushweller, C. H. *J. Am. Chem. Soc.* **1985**, *107*, 7823. Brunelle, J. A.; Bushweller, C. H.; English, A. D. *J. Phys. Chem.* **1976**, *80*, 2598.

in the AG and GG conformations were calculated by using the general dihedral angle driver method. As a calibration, the methyl rotation barrier in trimethylamine was calculated to be 4.37 kcal/mol. This is in excellent agreement with the experimental value (4.41 kcal/mol).[5] The various calculated barriers are compiled in Table II. The barriers range from 2.96 to 4.24 kcal/mol. Assuming an entropy of activation equal to zero, the highest calculated methyl rotation barrier gives a rate at 95 K that is about 4-5 times faster than that for the AG to GG conversion. It is possible that slowing methyl rotation contributes to additional exchange broadening of the ^1H DNMR line shape at or below 100 K.

Summary

Both the ^1H and $^{13}C\{^1H\}$ NMR spectra of isopropyldimethylamine decoalesce at very low temperatures and, at about 94 K, show two different subspectra. The major subspectrum (72-77%) is assigned to the C_1-symmetric enantiomers that have one isopropyl methyl group anti and the other gauche to the lone pair (AG and GA conformations). The minor subspectrum (23-28%) is assigned to the C_s-symmetric GG conformer that has both isopropyl methyl groups gauche to the lone pair; the methine proton is anti to the lone pair. At about 94 K, the AG (or GA) conformer is preferred over the GG form by a free energy difference of 0.07 ± 0.02 kcal/mol. Theoretical simulations of the exchange-broadened NMR spectra indicate a preferred (lowest barrier) AG to GG to GA conformational-exchange pathway. The free energy of activation for the AG (or GA) to GG process is 4.5 kcal/mol at 95 K. This is one of the lowest barriers measured by using NMR spectroscopy. The lower limit value of the free energy of activation for the AG to GA conversion is estimated to be 5.2 kcal/mol. Molecular mechanics calculations using Allinger's 1987 MM2 force field are in substantial agreement with the experimental results indicating that there is an enthalpy preference of 0.19 kcal/mol for the GG conformation and a barrier (ΔH^*) for the AG to GG process (5.37 kcal/mol) that is lower than that for the AG to GA conversion (7.84 kcal/mol). Calculated barriers for isolated methyl rotation range from 2.96 to 4.24 kcal/mol.

Experimental Section

NMR Spectra. The NMR spectra were recorded by using a Bruker WM-250 NMR system equipped with an Aspect 3000 computer. The magnet pole gap was modified to allow safe operation (no magnet O-ring freezing) down to 93 K. NMR sample temperature was varied by using a custom-built cold nitrogen gas delivery system used in conjunction with the Bruker BVT-1000 temperature control unit. Temperature measurement is accurate to ±3 K. NMR samples were prepared in precision 5- or 10-mm tubes and sealed after four freeze-pump-thaw cycles. All spectra are referenced to tetramethylsilane at 0 ppm.

Isopropyldimethylamine (IDMA). IDMA was prepared by using the procedure of Clark, Gillespie and Weisshaus[22] and purified on a 25% SF-96/5% XE-60 on Chromosorb WAW GLC column (20 ft × $^3/_8$ in.) at 413 K. NMR data: see DNMR Studies and Discussion.

Isopropyldi(methyl-d_3)amine. With cooling and stirring, 54 g (0.62 mol) of isopropylamine was neutralized by the slow addition of concentrated hydrochloric acid. The water was removed under vacuum, leaving the solid amine hydrochloride. The amine hydrochloride was dissolved in 50 mL of D_2O (99.9% isotopic purity, Cambridge Isotopes) and refluxed for 5 h under an efficient condenser equipped with a drying tube. The water was then removed under vacuum. This procedure was repeated seven times to give $(CH_3)_2CHND_3Cl$ that is 98.6% isotopically pure by NMR analysis. With cooling, the sample of $(CH_3)_2CHND_3Cl$ was neutralized (pH > 10) by the slow addition of 40% NaOD in D_2O (99.5% isotopically pure, Cambridge Isotopes). The resulting mixture was extracted with four 40-mL portions of anhydrous ether. The ether extracts containing $(CH_3)_2CHND_2$ were combined, dried over anhydrous Na_2SO_4, and filtered. Employing a modification of the procedure of Clark, Gillespie and Weisshaus,[22] we added 3.1 g (0.053 mol) of formic acid-d_2 (98% isotopically pure, 95% in D_2O, Cambridge Isotopes) with cooling to the ether solution of $(CH_3)_2CHND_2$. The ether, excess amine, and D_2O were removed first by careful distillation and then under vacuum to yield a viscous yellow oil. An additional 3.1-g (0.053-mol) sample of formic acid-d_2 and 100 mL of a 20% solution of formaldehyde-d_2 (98% isotopically pure, Cambridge Isotopes) were added to the yellow oil. The mixture was allowed to reflux for 24 h, acidified with 10 mL of concentrated HCl, and pumped under vacuum to yield a moist solid. With cooling, 40% NaOH in water was added dropwise to pH > 10. The aqueous layer was extracted with four 10-mL portions of ether and the ether dried over anhydrous Na_2SO_4. Isopropyldimethyl-$d_3$amine was purified on a 25% SF-96/5% XE-60 on Chromosorb WAW GLC column (20 ft × $^3/_8$ in.) at 413 K. ^1H NMR (CCl_4): δ 2.52 (1 H, septet, $^3J_{HH}$ = 6.1 Hz, CH), δ 0.96 (6 H, doublet, $C(CH_3)_2$), δ 2.08 (0.1 H, $N(CHD_2)_2$). Also see DNMR Studies and Discussion.

Acknowledgment. We are grateful to the University of Vermont Academic Computing Center for computational support.

Registry No. IDMA, 996-35-0.

(22) Clark, H.; Gillespie, H.; Weisshaus, S. *J. Am. Chem. Soc.* **1933**, *55*, 4571.

Picosecond Radical Kinetics. Rate Constants for Reaction of Benzeneselenol with Primary Alkyl Radicals and Calibration of the 6-Cyano-5-hexenyl Radical Cyclization

Martin Newcomb,*[1a] Thomas R. Varick,[1a] Chau Ha,[1a] M. Beata Manek,[1b] and Xu Yue[1b]

Contribution from the Departments of Chemistry, Wayne State University, Detroit, Michigan 48202, and Texas A&M University, College Station, Texas 77843.
Received April 27, 1992

Abstract: The cyclopropylcarbinyl radical ring opening was used as a radical clock to determine rate constants for benzeneselenol trapping in THF and in toluene. Hydrogen atom transfer trapping from PhSeH appeared to be partially diffusion controlled. An operational Arrhenius function for trapping in THF is log (k_T·M s) = 11.03 - 2.27/2.3RT. The recommended function for PhSeH trapping in other low-viscosity organic solvents is log (k_T·M s) = 10.87 - 2.10/2.3RT. The rate constant for trapping at 25 °C is 2.1 × 10^9 M^{-1} s^{-1}. The kinetic values are expected to apply for PhSeH trapping of simple primary alkyl radicals. As a check on this assumption, cyclization of the 6-cyano-5-hexenyl radical (**9**), produced from the corresponding PTOC ester radical precursor, was calibrated with PhSH and PhSeH trapping. The two trapping agents gave essentially equivalent results. The cyclizations of both (*E*)- and (*Z*)-**9** are described by log (k_r·s) = 11.0 - 3.8/2.3RT. This fast rearrangement (k_r = 1.6 × 10^8 s^{-1} at 25 °C) could prove to be useful as a radical clock for timing fast second-order processes.

Knowledge of the rates of radical reactions is important for mechanistic probe and radical clock studies. For very fast radical reactions, considerable progress in kinetic methodology has been reported in the past several years, especially for measurements

0002-7863/92/1514-8158$03.00/0